Switching of selectivity from benzaldehyde to benzoic acid using MIL-100(V) as a heterogeneous catalyst in aerobic oxidation of benzyl alcohol

Duygu Hacıefendioğlu[1,2], Ali Tuncel[1,*]

[1]Hacetepe University, Chemical Engineering Department, Ankara/Turkey

[2]Hacettepe University, Graduate School of Science and Engineering, Chemical Engineering Department, Ankara/Turkey

*: Corresponding author: Dr. Ali Tuncel (atuncel@hacettepe.edu.tr)

Supporting Information

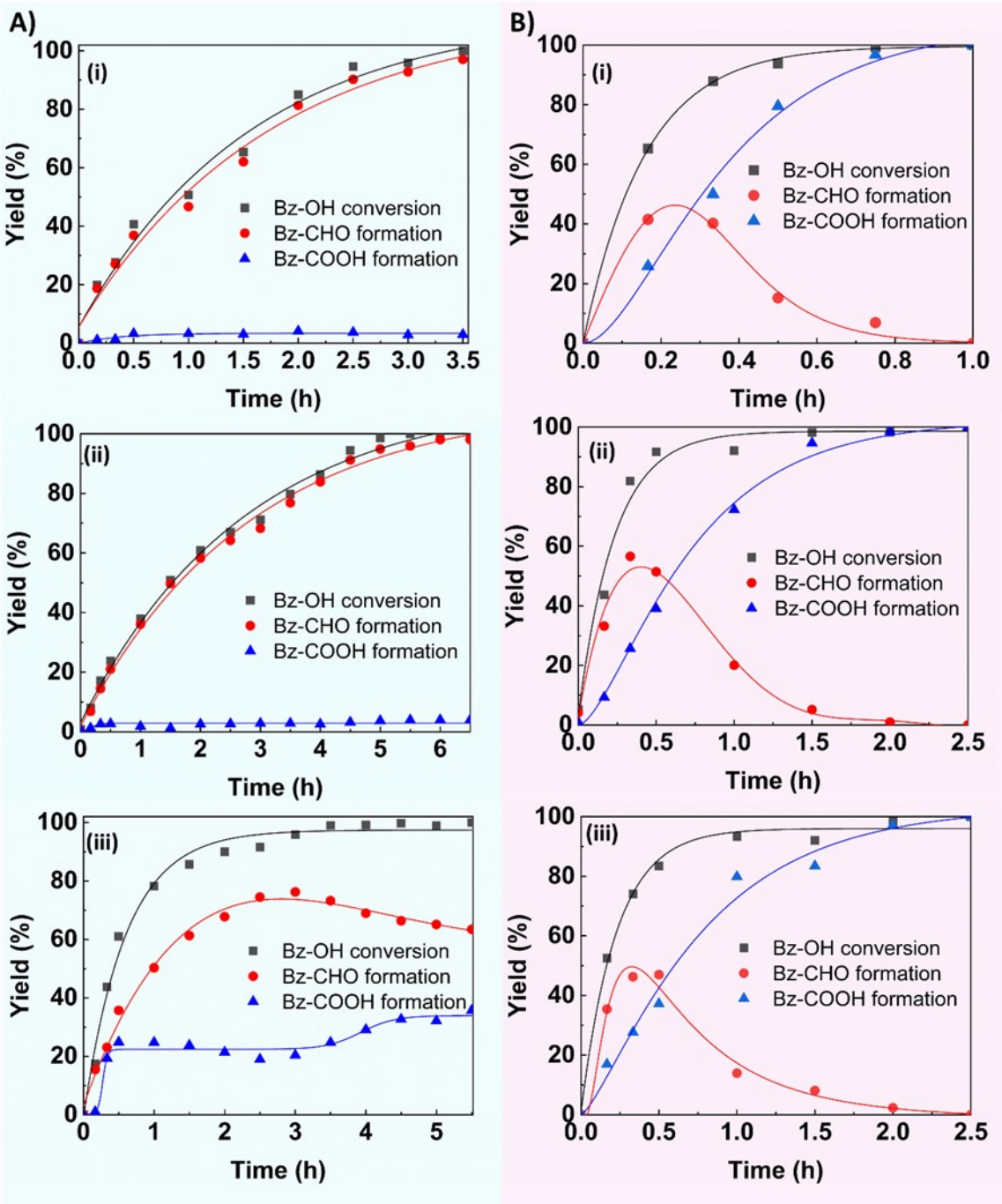

Figure S1. The variation of Bz-CHO and Bz-COOH formations with the time in the Bz-OH oxidations performed by changing initial Bz-OH concentration at 80°C and 120°C, using molecular oxygen as the oxidant. (A) Bz-CHO and Bz-COOH formation profiles at 80°C, Bz-OH concentration (mM): (i) 48.1, (ii) 96.2, (iii) 192.4, (B) Bz-CHO and Bz-COOH formation profiles at 120°C, Bz-OH concentration (mM): (i) 48.1, (ii) 96.2, (iii) 192.4, Common conditions: DEGDME: 2.5 mL, O_2 flow rate: 0.015 L/min, MIL-100(V) concentration for the runs performed at 80°C: 32 mg/mL, MIL-100(V) concentration for the runs performed at 120°C: 8 mg/mL.

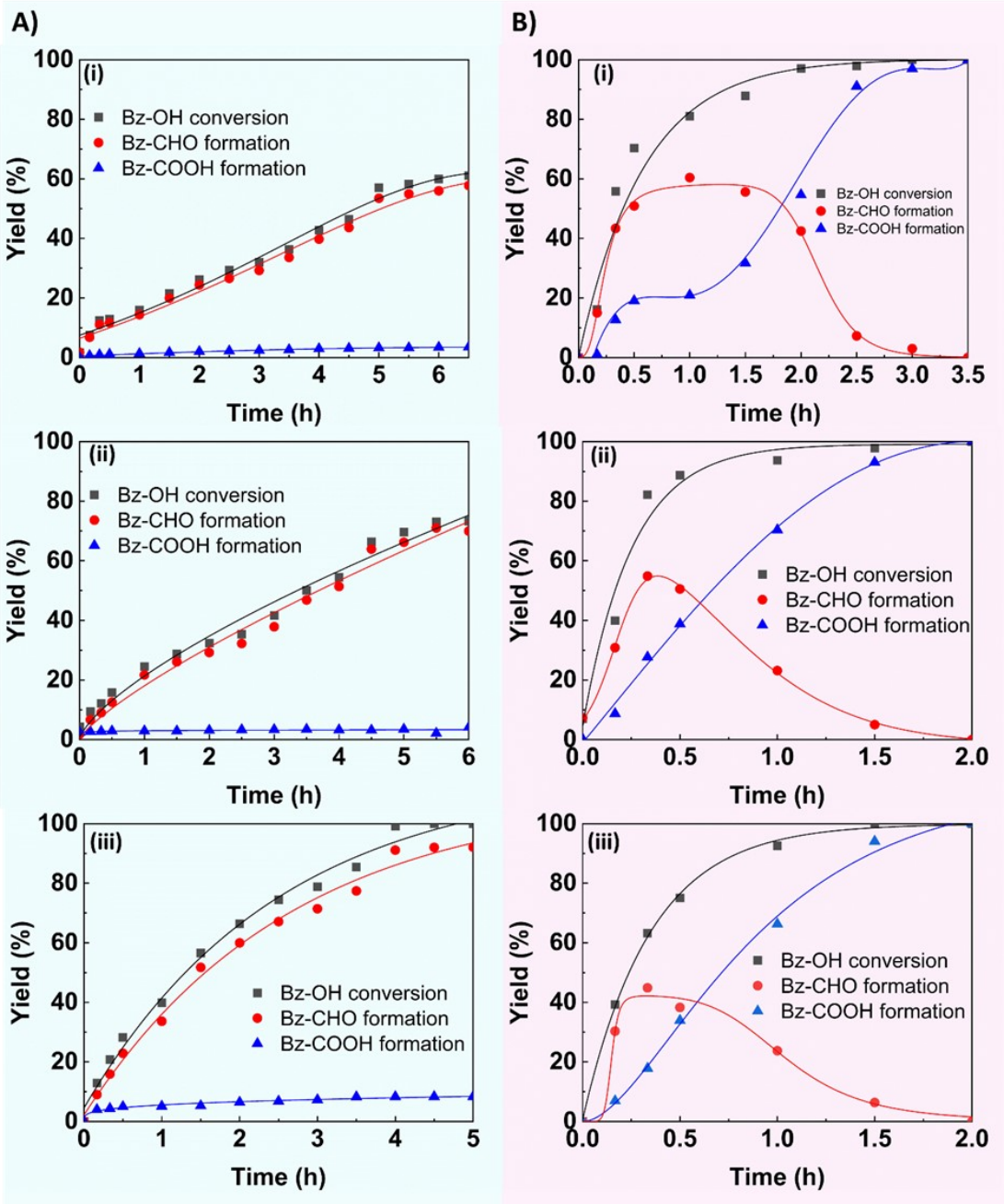

Figure S2. The variation of Bz-CHO and Bz-COOH formations with the time in the Bz-OH oxidations performed by changing air flow rate at 80°C and 120°C. (A) Bz-CHO and Bz-COOH formation profiles at 80°C, Air flow rate (L/min): (i) 0.05, (ii) 0.075, (iii) 0.150, (B) Bz-CHO and Bz-COOH formation profiles at 120°C, Air flow rate (L/min): (i) 0.05, (ii) 0.075, (iii) 0.150, Common conditions: DEGDME: 2.5 mL, MIL-100(V) concentration for the runs performed at 80°C: 32 mg/mL, MIL-100(V) concentration for the runs performed at 120°C: 8 mg/mL.

Table S1. The comparison of TOF values obtained for this study with the those obtained with different catalysts synthesized for oxidation of benzyl alcohol.

Catalyst	Oxidation agent	Temperature	Catalyst/Bz-OH ratio (mol/mol)	TOF(h^{-1})	Reference
Pd/CeO_2	O_2	120°C	0.009	350000[a,b,c]	S1
PA-Na-1	O_2	140°C	0.0001	106200[a,b,c,d]	S2
In_2O_3@Pd/MCF-H_2	O_2	110°C	0.03	49400[a,c,d]	S3
Au/Mg_3Al-L	O_2	80°C	0.002	2615[a,b,e]	S4
Au/S1CNT	O_2	50°C	0.002	2294[a,b,e]	S5
Pd/CeO_2-R	O_2	90°C	0.0002	1290[c]	S6
Au_xPd_y/CNT	O_2	80°C	0.007	1274[a,b]	S7
Pd-IL-HNTs	H_2O_2	70°C	20 mg/2.88mmol	118.1[a,b]	S8
Pt/5MnNS	O_2	25°C	0.09	1.8[a]	S9
SO_4^{-2}/Zr-OMC	TBHP	90°C	0.099	34668[a,b,d]	S10
Fe_{SA}/MoS_2	O_2	120 °C	0.001	2105[f]	S11
Cu_xO_y@PCNs-H_2O_2	TBHP	80°C	0.018	535.5[a,b]	S12
[{VO(OEt)(EtOH)}2(L2)]	TBHP	RT	0.002	389[f]	S13
AuSn/rGO-CoIM	O_2	100°C	0.018	103.6[a,e]	S14
MOF-BASU1	TBHP	80°C	0.008	77.6[f]	S15
[Mn(bipy)2]2+HMS	TBHP	90 °C	0.0013	21.28[f]	S16
Im-Tpy@Co	Air	RT	0.2	34.17[f]	S17
Co@NC	O_2	60°C	0.046	15.6[f]	S18
VO_x@SiO_2	PMS	25°C	0.025	0.075[a,d]	S19
MIL-100(V)	O_2	120°C	0.001	497[f]	**This work**
MIL-100(V)	O_2	80°C	0.006	68.3[f]	**This work**

a: Based on Bz-OH conversion, b: Based on metal surface dispersion, c: Based on only Pd, d: Calculated from the data reported in the reference, e: Based on only Au, f: TOF= $n_{Main\ product}$ / ($n_{vanadium}$x$t_{reaction}$) where $n_{Main\ product}$ is the mole of main product, $n_{vanadium}$: mole of vanadium in MIL-100 (V), $t_{reaction}$: is the reaction period for obtaining 80 % of Bz-OH conversion.

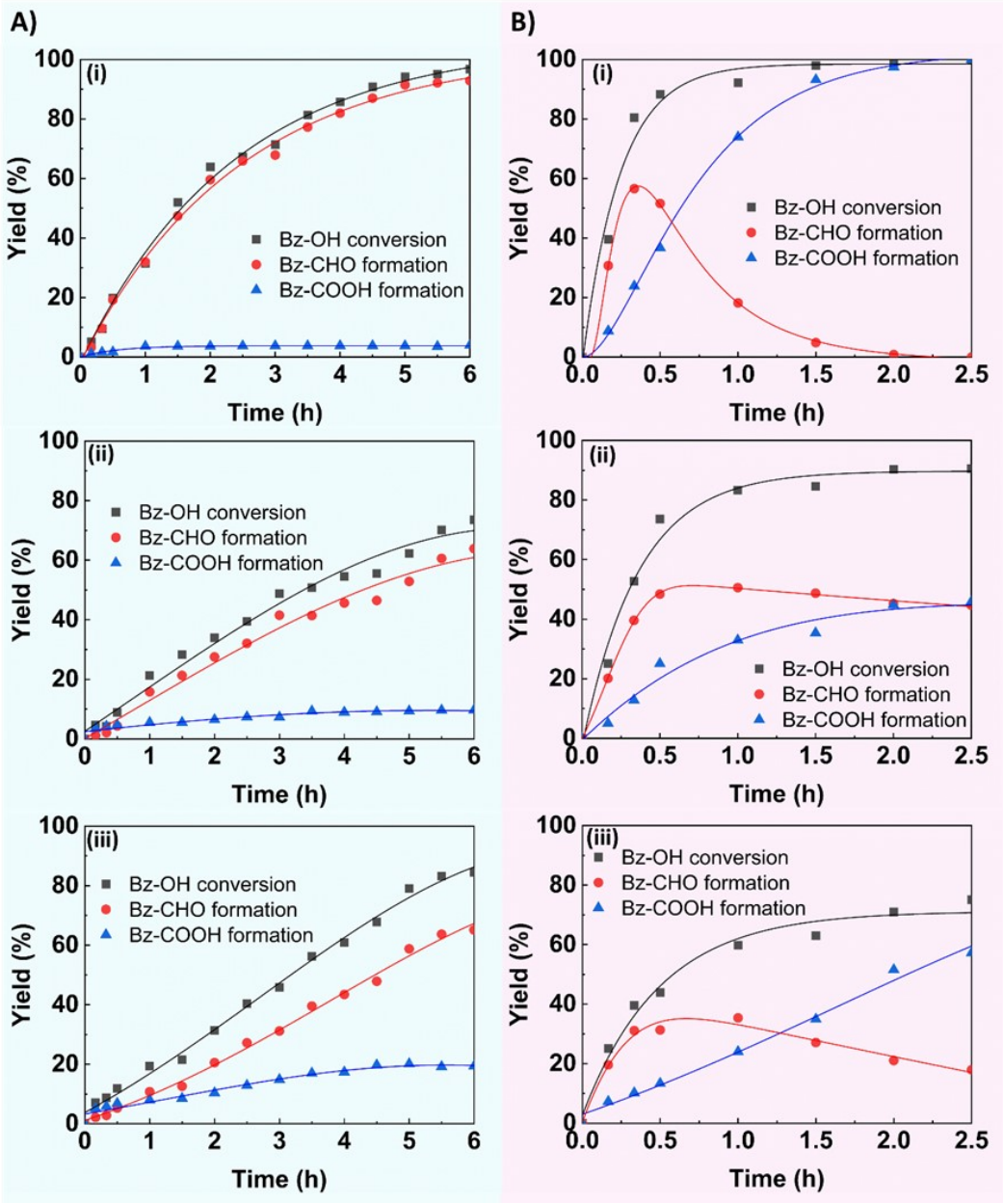

Figure S3. The variation of Bz-CHO and Bz-COOH formations with the time in the Bz-OH oxidations performed using different radical scavengers at two different reaction temperatures. Temperature and type of radical scavenging agent: (A) Bz-CHO and Bz-COOH formation profiles at 80°C, Scavenger type: (i) L-AA, (ii) IPA, (iii) NaN_3, (B) Bz-CHO and Bz-COOH formation profiles at 120°C, Scavenger type: (i) L-AA, (ii) IPA, (iii) NaN_3, Common conditions: Bz-OH initial concentration: 98.2 mM, O_2 flow rate: 0.015 L/min, DEGDME: 2.5 mL, MIL-100(V) concentration for the runs performed at 80°C: 32 mg/mL, MIL-100(V) concentration for the runs performed at 120°C: 8 mg/mL.

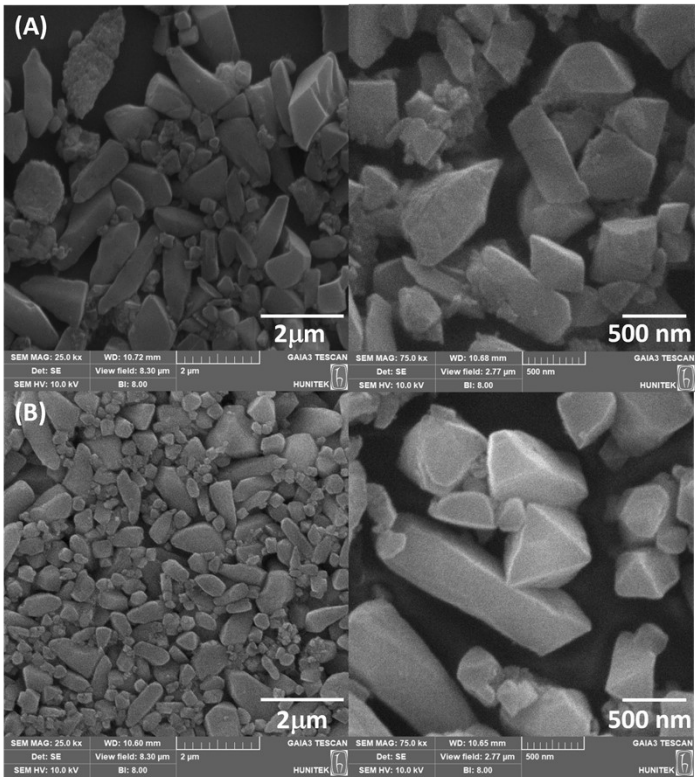

Figure S4. The SEM photographs of MIL-100(V) (A) after using five consecutive Bz-OH oxidation runs at 80°C, (B) after using five consecutive Bz-OH oxidation runs at 120°C. Common conditions: Bz-OH initial concentration: 98.2 mM, O_2 flow rate: 0.015 L/min, DEGDME: 2.5 mL, MIL-100(V) concentration for the runs performed at 80°C: 32 mg/mL, MIL-100(V) concentration for the runs performed at 120°C: 8 mg/mL.

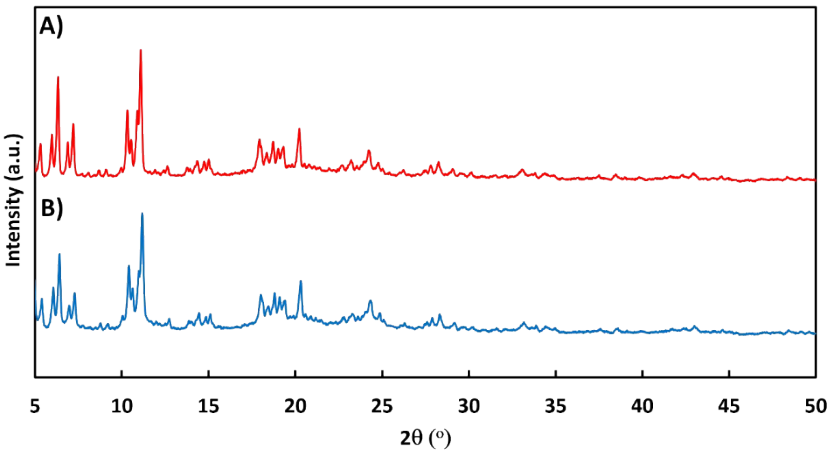

Figure S5. X-ray diffraction spectra of MIL-100(V) after using five consecutive Bz-OH oxidation runs performed at (A) 80°C and (B) 120°C. The reaction conditions are given in **Figure S4**.

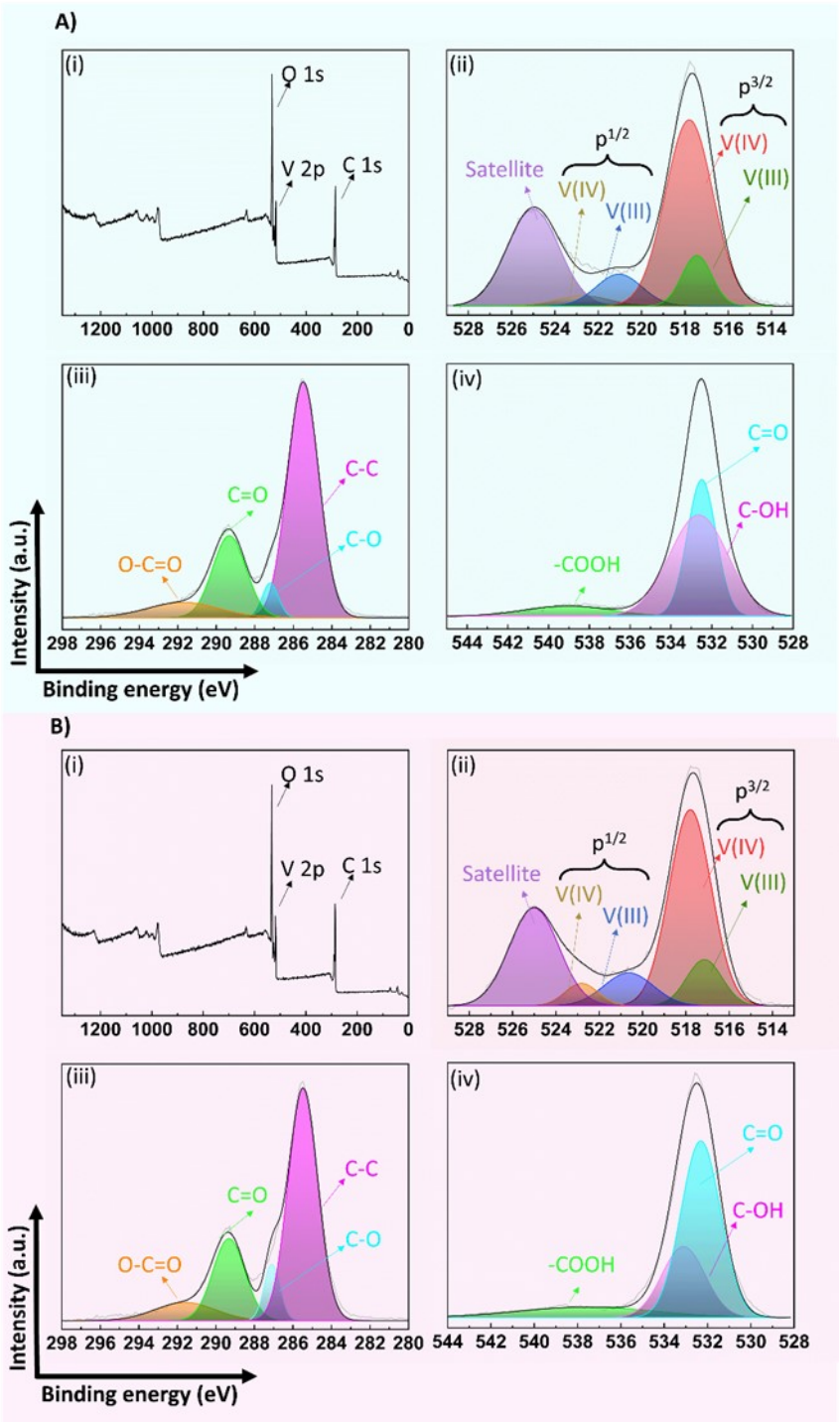

Figure S6. X-ray photoelectron spectroscopy of MIL-100(V) after using five consecutive Bz-OH oxidation runs at 80°C. (A): (i) Survey XPS spectrum, Core level spectra for (ii) V 2p scan, (iii) C 1s scan, (iv) O 1s scan. Bz-OH oxidation conditions are given in Figure 9. X-ray photoelectron spectroscopy of MIL-100(V) after using five consecutive Bz-OH oxidation runs at 120°C. (B): (i) Survey XPS spectrum, Core level spectra for (ii) V 2p scan, (iii) C 1s scan, (iv) O 1s scan. The reaction conditions are given in **Figure S4**.

References

[S1] Z. Wang, B. Zhang, S. Yang, X. Yang, F. Meng, L. Zhai, Z. Li, S. Zhao, G. Zhang, Y. Qin, Dual Pd^{2+} and Pd^{0} sites on CeO_2 for benzyl alcohol selective oxidation, J. Catal. 414 (2022) 385-393. https://doi.org/10.1016/j.jcat.2022.09.012.

[S2] H. Yuan, Q. Li, Z. Liu, Q. Qi, C. Wan, X. Yin, X. Yang, Y. Ding, Z. Du, Solvent-free efficient oxidation of benzyl alcohol on nano-Pd/Al_2O_3: Effect of palladium source and pH value, Appl. Catal. A 654 (2023) 119070. https://doi.org/10.1016/j.apcata.2023.119070.

[S3] P. Bai, Z. Zhao, Y. Zhang, Z. He, Y. Liu, C. Wang, S. Ma, P. Wu, L. Zhao, S. Mintova, Z. Yan, rational design of highly efficient PdIn–In_2O_3 interfaces by a capture-alloying strategy for benzyl alcohol partial oxidation, ACS Appl. Mater. Interfaces 15 (2023) 19653-19664. https://doi.org/10.1021/acsami.3c00810.

[S4] J. Luo, S. Yang, Y. Ling, W. Yang, H. Niu, W. Li, H. Liu, C. Liang, Defective Au nanoparticles manipulated by Au-MgxAl-LDH interplay for alkali-free oxidation of benzyl alcohol, J. Chem. Eng. 473 (2023) 145171. https://doi.org/10.1016/j.cej.2023.145171.

[S5] J. Luo, Y. Dong, S. Yang, F. Shan, Q. Jiang, Y. Ma, C. Liang, Au nanoparticles anchored on sulfonated carbon nanotubes for benzyl alcohol oxidation, ACS Appl. Nano Mater. 4 (2022) 4887-4895. https://doi.org/10.1021/acsanm.1c04453.

[S6] L. Zhang, R. Chen, Y. Tu, X. Gong, X. Cao, Q. Xu, Y. Li, B. Ye, Y. Ye J. Zhu, Revealing the crystal facet effect of ceria in Pd/CeO_2 catalysts toward the selective oxidation of benzyl alcohol, ACS Catal. 13 (2023) 2202-2213. https://doi.org/10.1021/acscatal.2c04252.

[S7] J. Luo, Y. Zhou, S. Yang, W. Zhu, S. Li, C. Liang, structural construction of Au–Pd nanocomposite for alkali-free oxidation of benzyl alcohol, ACS. Appl. Mater. Interfaces 15 (2023) 22025-22035. https://doi.org/10.1021/acsami.3c00163.

[S8] J. Wang, Y. Zhang, Y. Xu, P. Zhang, Q. Gao, Q. Liang, W. Zhang, W. Li, R. Guo, B. Jin, S. Miao, Halloysite-based nanomotors with embedded palladium nanoparticles for

selective benzyl alcohol oxidation, ACS Appl. Nano Mater. 5 (2022) 12806-12816. https://doi.org/10.1021/acsanm.2c02686.

[S9] Y Shi, M. Shen, Z. Wang, C. Liu, J. Bi, L. Wu, Visible-light-driven benzyl alcohol oxidation over Pt/Mn-$Bi_4Ti_3O_{12}$ nanosheets: Structure-function relationship of multicomponent photocatalysts, J. Catal. 418 (2023) 141-150. https://doi.org/10.1016/j.jcat.2023.01.015.

[S10] A. Ramesh, R. Manigandan, B. M. Ali, K. Dhandapani, C. T. Da, M.T.N. Le, Selective oxidation of benzyl alcohol over sulphated zirconia incorporated ordered mesoporous carbon by a hard template method, J. Alloys Compd. 918 (2022) 165729. https://doi.org/10.1016/j.jallcom.2022.165729.

[S11] Z. Li, H. Li, Z. Yang, X. Lu, S. Ji, M. Zhang, J. H. Horton, H. Ding, Q. Xu, J. Zhu, J. Yu, Facile synthesis of single iron atoms over MoS_2 nanosheets via spontaneous reduction for highly efficient selective oxidation of alcohols, Small, 18 (2022) 2201092. https://doi.org/10.1002/smll.202201092.

[S12] J. Liu, H. Yang, U. I. Kara, E. Boerner, Y. Luo, H. Yu, Y. Xu, X. Wang, K. Huang, A facile synthesis of stable copper-based core-shell catalysts for highly efficient 4-nitrophenol reduction and benzyl alcohol oxidation, J. Chem. Eng. 479 (2024) 147778. https://doi.org/10.1016/j.cej.2023.147778.

[S13] M. Sutradhar, M. G. Martins, D.H.B.G.O.R. Simões, R. M.N. Serôdio, H. M. Lapa, E.C.B.A. Alegria, M.F. C. G. da Silva, A. J.L. Pombeiro, Ultrasound and photo-assisted oxidation of toluene and benzyl alcohol with oxidovanadium(V) complexes, Appl. Catal. A. 638 (2022) 118623. https://doi.org/10.1016/j.apcata.2022.118623.

[S14] L. Liu, X. Zhou, C. Xin, B.Zhang, G. Zhang, S. Li, L. Liu, X. Tai, Efficient oxidation of benzyl alcohol into benzaldehyde catalyzed by graphene oxide and reduced graphene oxide supported bimetallic Au–Sn catalysts, RSC Adv. 13 (2023) 23648-23658. https://doi.org/10.1039/D3RA03496H.

[S15] M. Yaghubzadeh, S. Alavinia, R. G. Vaghei, A sustainable protocol for selective alcohols oxidation using a novel iron-based metal organic framework (MOF-BASU1), RSC Adv. 13 (2023) 24639-24648. https://doi.org/10.1039/d3ra03058j.

[S16] V. Mahdavi, M. Mardani, Selective oxidation of benzyl alcohol with tert-butylhydroperoxide catalysed via Mn (II) 2, 2-bipyridine complexes immobilized over the mesoporous hexagonal molecular sieves (HMS), J. Chem. Sci. 124 (2012) 1107-1115. https://doi.org/10.1007/s12039-012-0307-4.

[S17] S. Kumar, M. Kumar, V. Bhalla, Cobalt-centered supramolecular nanoensemble for regulated aerobic oxidation of alcohols and “one-pot” synthesis of quinazolin-4(3h)-ones, ACS Appl. Mater. Interfaces, 15 (2023) 49246-49258. https://doi.org/10.1021/acsami.3c11244.

[S18] Q. Hao, Z. Li, Y. Shi, R. Li, Y. Li, L. Wang, H. Yuan, S. Ouyang, T. Zhang, Plasmon-induced radical-radical heterocoupling boosts photodriven oxidative esterification of benzyl alcohol over nitrogen-doped carbon-encapsulated cobalt nanoparticles, Angew. Chem. Int. Ed. 62 (2023) e202312808. doi.org/10.1002/anie.202312808.

[S19] Y. Wu, L.H. Kong, W.T. Ge, W.J. Zhang, Z.Y. Dong, X.J. Guo, X. Yan, Y. Chen, W.Z. Lang, A porous V/SiO_2 sphere composite for the selective oxidation of benzyl alcohol to benzaldehyde in aqueous phase through peroxymonosulfate activation, J. Catal, 413 (2022) 668-680. https://doi.org/10.1016/j.jcat.2022.07.011.